Electronic supplementary information (ESI) for

Metal–Semiconductor–Metal Ternary Heteronanocrystals with Multiple Plasmonic Effects for Efficient Photocatalysis

Dae Han Wi,‡[a] Hyunwoo Yang,‡[a] Yonghyeon Kim,‡[a] Hojin Ahn,[a] Jong Wook Hong,*[b] and Sang Woo Han*[a]

[a]Center for Nanotectonics, Department of Chemistry and KI for the NanoCentury, KAIST, Daejeon 34141, Korea. E-mail: sangwoohan@kaist.ac.kr

[b]Department of Chemistry, University of Ulsan, Ulsan 44776, Korea. E-mail: jwhong@ulsan.ac.kr

‡These authors contributed equally to this work.

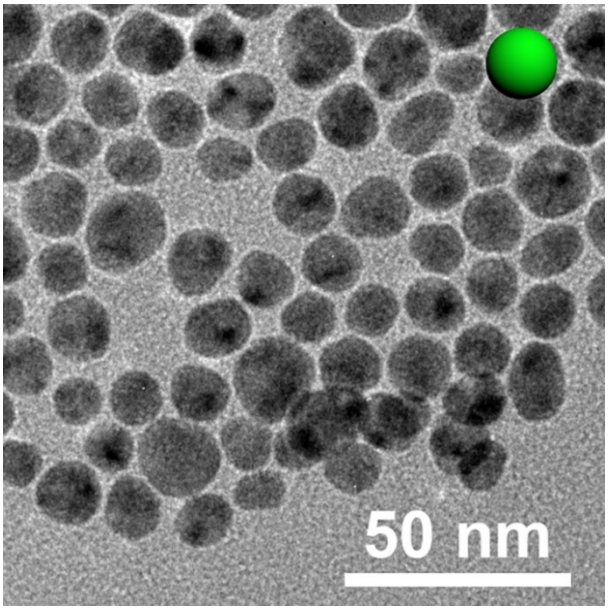

Fig. S1 TEM image of Ag NCs. Inset shows a three-dimensional geometric model of Ag NCs. The average size of Ag NCs was 11.9 ± 1.5 nm.

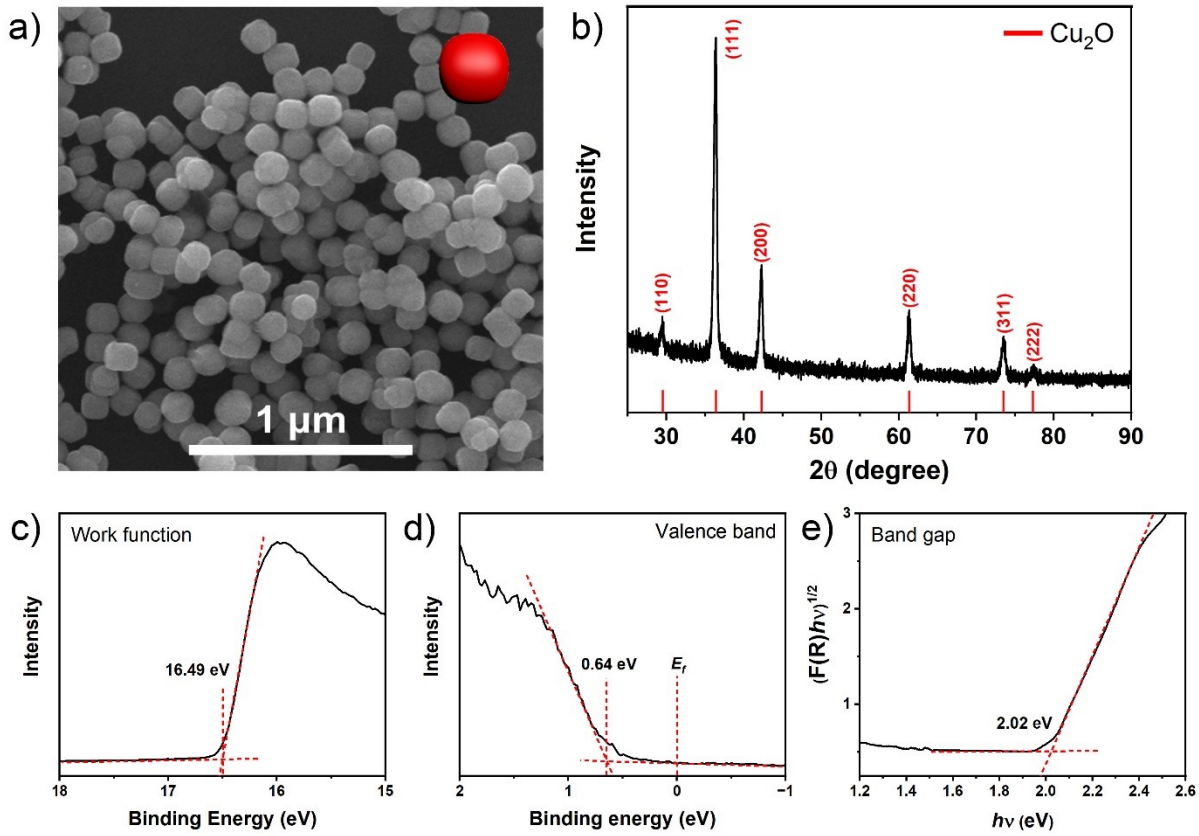

Fig. S2 (a) SEM image of Cu_2O NCs. Inset shows a three-dimensional geometric model of Cu_2O NCs. The average size of Cu_2O NCs was 123 ± 9 nm. (b) XRD pattern of Cu_2O NCs. The positions of Cu_2O reference were taken from the ICDD database (00-005-0667). The XRD pattern corroborates the cuprite structure of Cu_2O NCs. Ultraviolet photoelectron spectroscopy spectra of Cu_2O NCs for the estimation of their (c) work function and (d) valence band position. The work function of Cu_2O NCs was calculated to be 4.71 eV [incident photon energy (21.2 eV) – secondary electron cut-off (16.49 eV)], and the valence band position of Cu_2O NCs was 0.64 eV with respect to the Fermi level (E_f). (e) Tauc plot of Cu_2O NCs obtained with diffuse reflectance spectroscopy measurements. The band gap energy of Cu_2O NCs was estimated to be 2.02 eV. Accordingly, the conduction band position of Cu_2O NCs was calculated to be 3.33 eV.

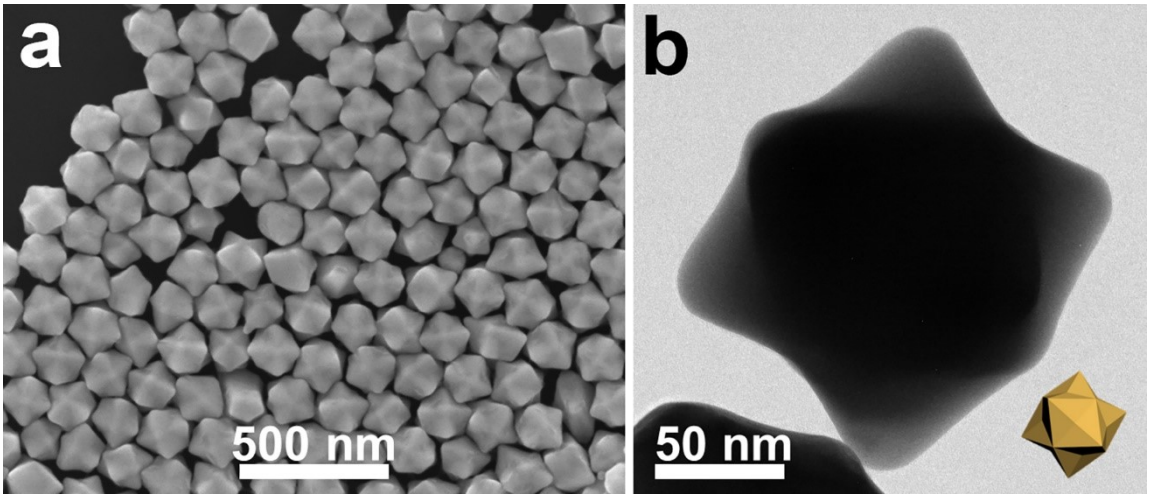

Fig. S3 (a) SEM and (b) TEM images of HOH Au NCs. Inset in b shows a three-dimensional geometric model of HOH Au NCs. The SEM-determined average size of HOH Au NCs was 136 ± 6 nm.

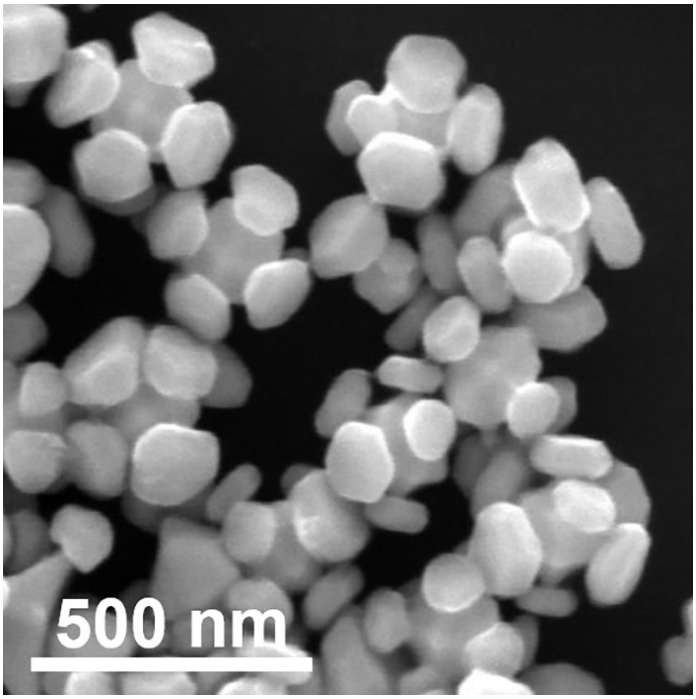

Fig. S4 SEM image of Au_{vertex}–Ag HNCs prepared by the reduction of $AgNO_3$ on HOH Au NCs in the presence of PVP.

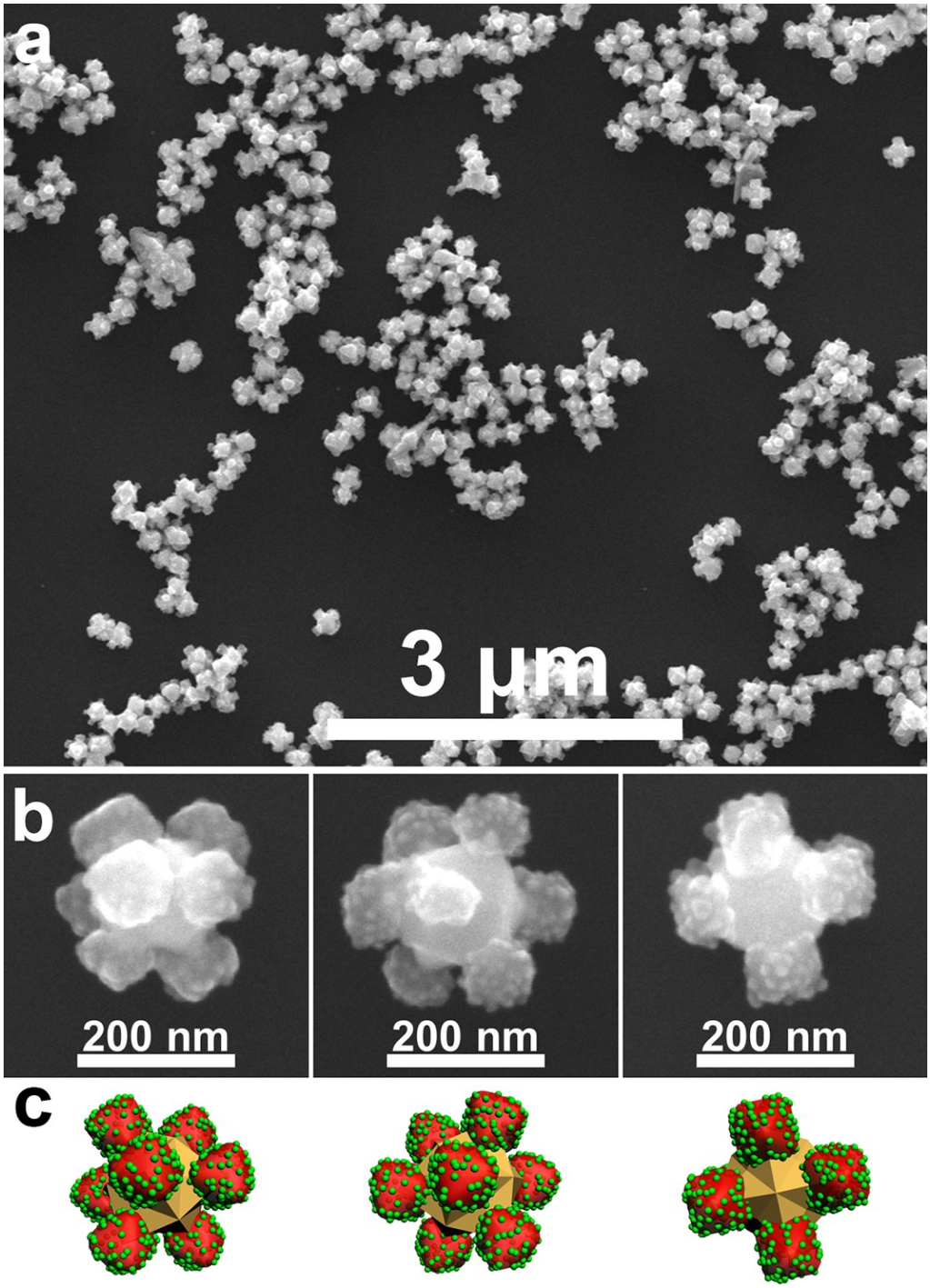

Fig. S5 (a) Low-magnification SEM image of Au_{vertex}–Cu_2O–Ag HNCs. (b) High-magnification SEM images and (c) corresponding three-dimensional geometric models of Au_{vertex}–Cu_2O–Ag HNCs viewed along different directions.

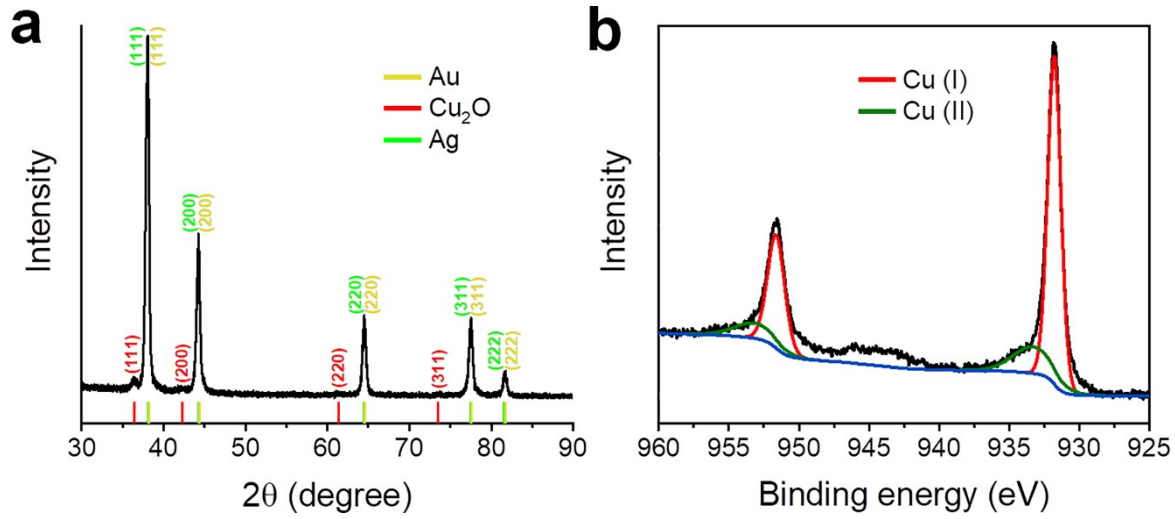

Fig. S6 (a) XRD pattern of Au_{vertex}–Cu_2O–Ag HNCs. The positions of Au, Cu_2O, and Ag references were taken from the ICDD database (Au: 00-004-0784, Cu_2O: 00-005-0667, Ag: 00-004-0783). (b) Cu 2p XPS spectrum of Au_{vertex}–Cu_2O–Ag HNCs.

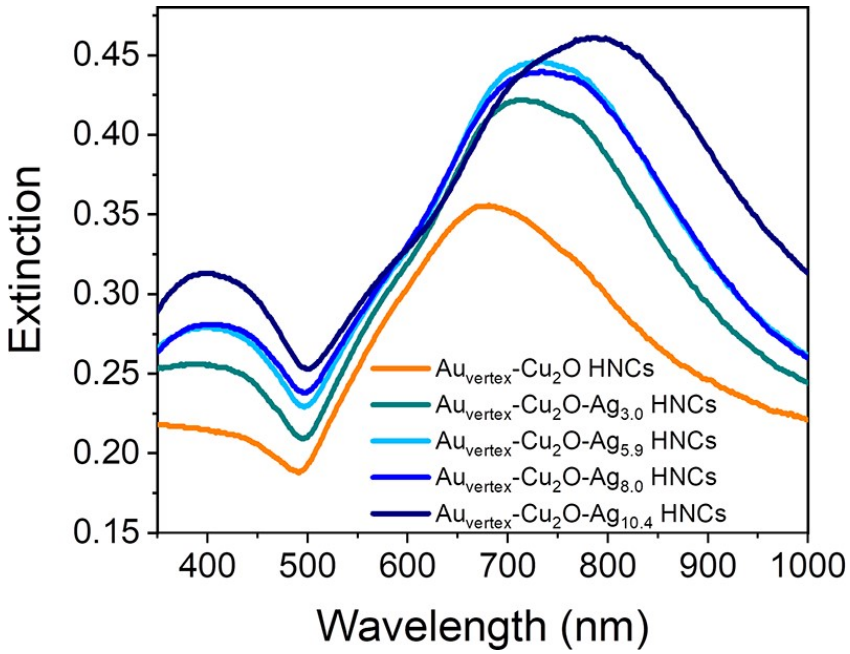

Fig. S7 Extinction spectra of Au_{vertex}–Cu_2O and Au_{vertex}–Cu_2O–Ag HNCs.

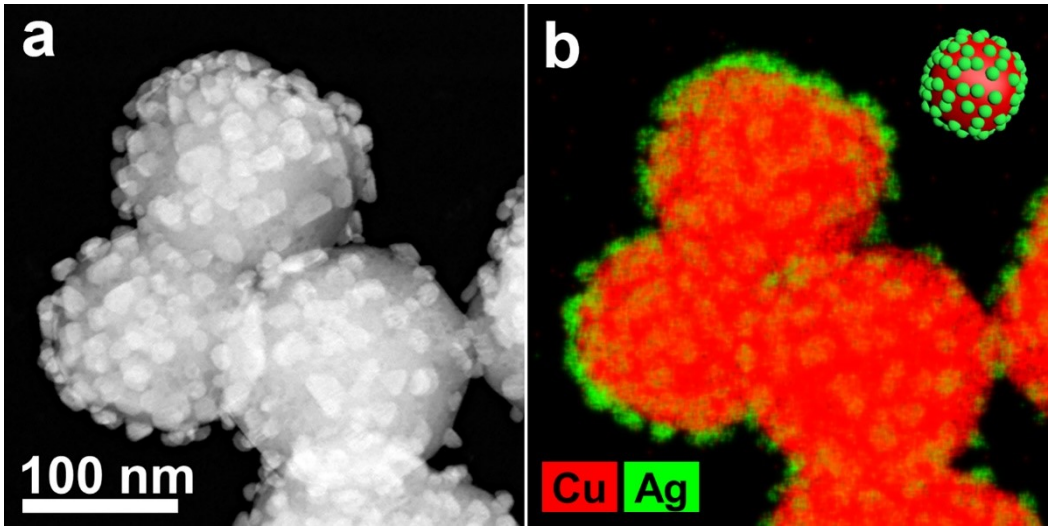

Fig. S8 (a) HADDF–STEM and (b) corresponding EDS elemental mapping images of Cu_2O–Ag HNCs. Inset in b shows a three-dimensional geometric model of Cu_2O–Ag HNCs.

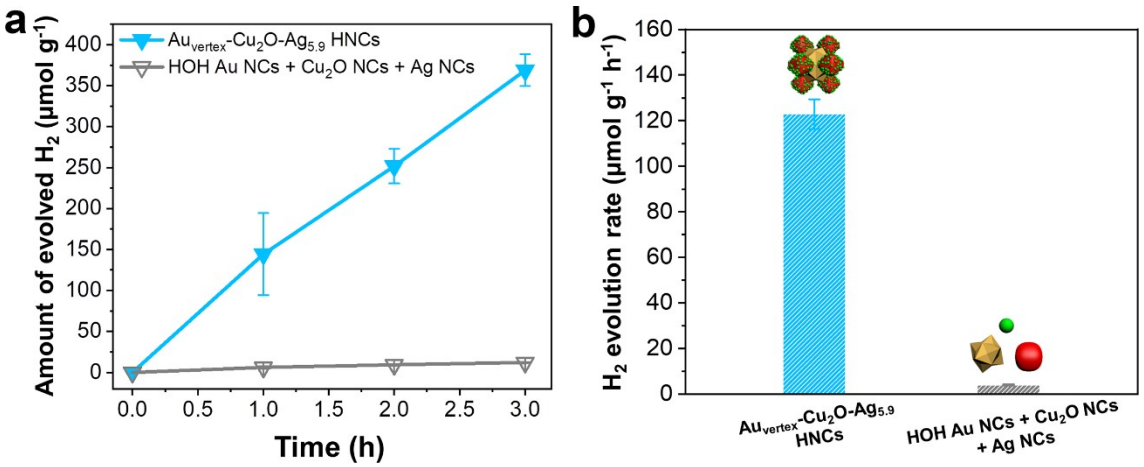

Fig. S9 (a) Amounts of H_2 evolved during the photocatalysis and (b) corresponding H_2 evolution rates obtained with Au_{vertex}–Cu_2O–$Ag_{5.9}$ HNCs and a physical mixture of HOH Au NCs, Ag NCs, and Cu_2O NCs.

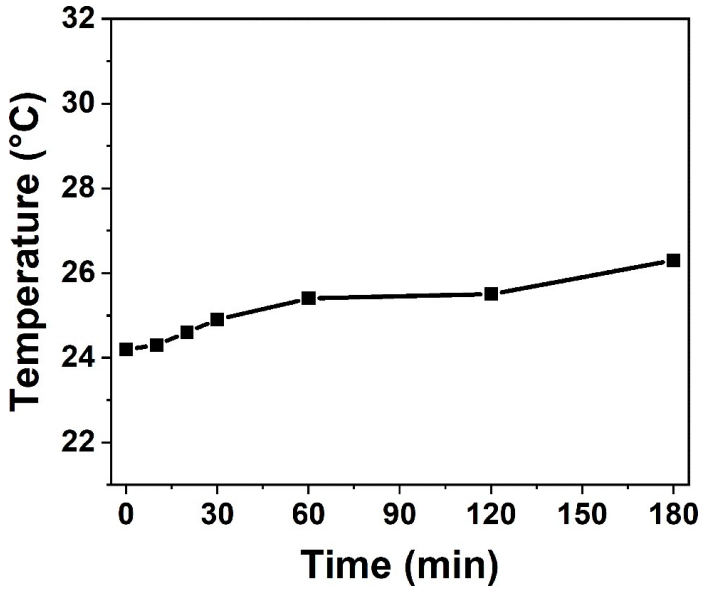

Fig. S10 Temperature of the reaction mixture during the photocatalysis for Au_{vertex}–Cu_2O–$Ag_{5.9}$ HNCs. The temperature was measured by inserting a thermometer (Summit Inc., TPI-330L) into the reaction cell.

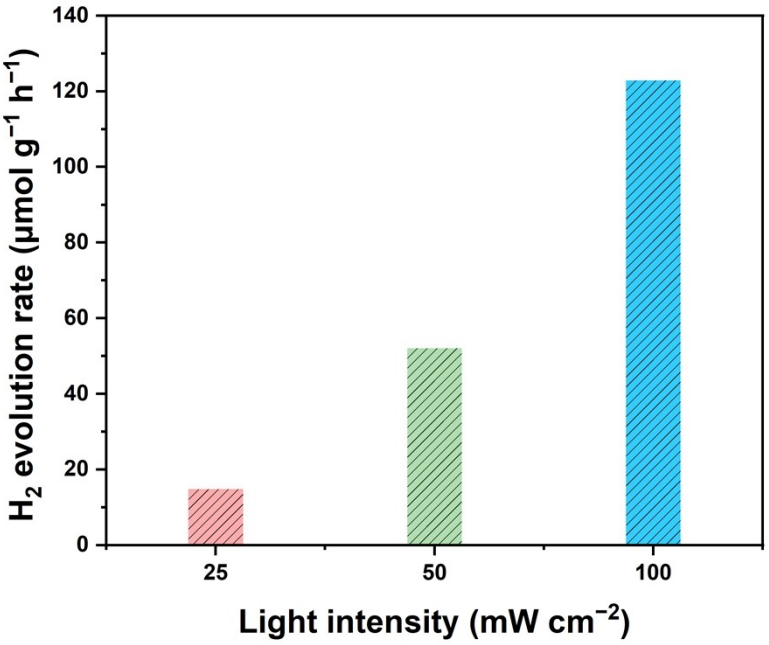

Fig. S11 Light intensity-dependent H_2 evolution rates of Au_{vertex}–Cu_2O–$Ag_{5.9}$ HNCs.

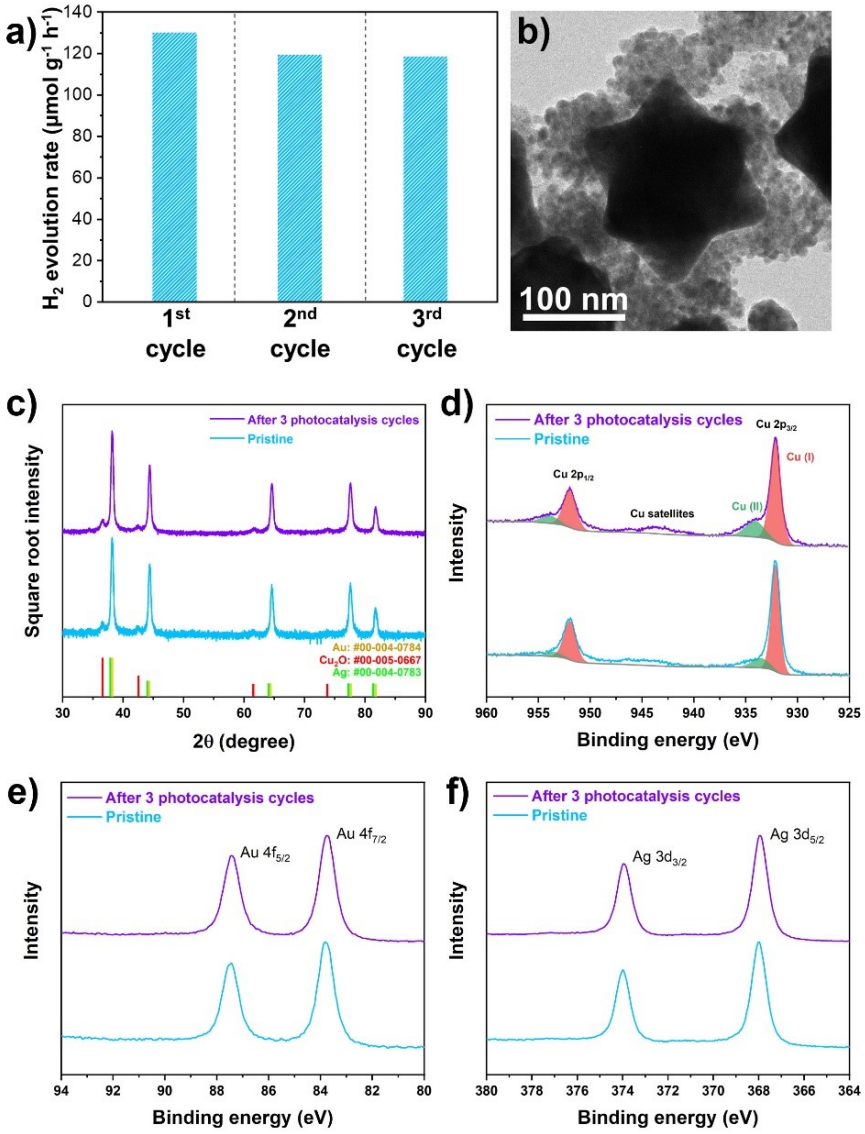

Fig. S12 (a) Recyclability of Au_{vertex}–Cu_2O–$Ag_{5.9}$ HNCs for photocatalytic H_2 evolution. Each photocatalysis cycle was conducted for 3 h. After each photocatalysis cycle, the catalysts were collected from the reaction solution by centrifuging and redispersed in a fresh aqueous methanol solution for the next photocatalysis cycle. The Au_{vertex}–Cu_2O–$Ag_{5.9}$ HNCs exhibited 91% H_2 evolution activity in the third cycle relative to that in the first cycle. The slight decrease in the activity during the recyclability test can be attributed to the loss of catalysts during the recollection process. (b) TEM image of Au_{vertex}–Cu_2O–$Ag_{5.9}$ HNCs obtained after the recyclability test, demonstrating no significant change in the morphology of the HNCs after the reaction. (c) XRD patterns and (d) Cu 2p XPS spectra of Au_{vertex}–Cu_2O–$Ag_{5.9}$ HNCs before and after the recyclability test. (e) Au 4f and (f) Ag 3d XPS spectra of Au_{vertex}–Cu_2O–$Ag_{5.9}$ HNCs before and after the recyclability test.

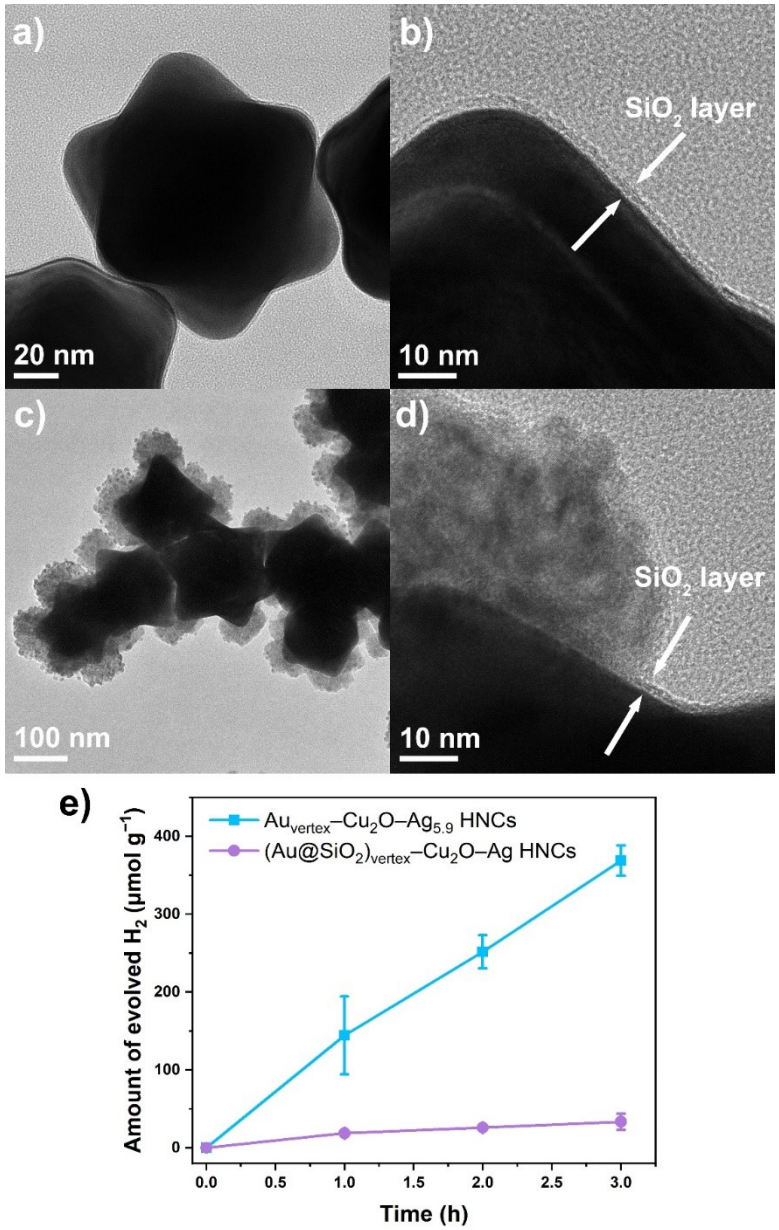

Fig. S13. TEM images of (a,b) HOH $Au@SiO_2$ core–shell NCs and (c,d) $(Au@SiO_2)_{vertex}$–Cu_2O–Ag HNCs. (e) Amounts of H_2 evolved during the photocatalysis with Au_{vertex}–Cu_2O–$Ag_{5.9}$ and $(Au@SiO_2)_{vertex}$–Cu_2O–Ag HNCs, which were normalized to the total mass of catalysts.

Table S1. Photocatalytic H_2 evolution rates of various Cu_2O-based photocatalysts.

Photocatalyst	Solvent	Light source	H_2 evolution rate ($\mu mol\ g^{-1}\ h^{-1}$)	Reference
Cu_2O cubes	0.5 M Na_2SO_3	300 W Xe lamp	4.6	*Angew. Chem. Int. Ed.*, 2018, **57**, 13613–13617
Multifaceted Cu_2O	0.0125 M glucose + 0.1M NaOH	300 W Xe lamp ($\lambda > 420$ nm)	18.83	*Chem. Commun.*, 2014, **50**, 192–194
Octahedral hexa-pod Cu_2O	pure water	300 W Xe lamp	7.14	*CrystEngComm*, 2010, **12**, 406–412
Pd/Cu_2O cubes	pure water	300 W Xe lamp ($\lambda > 400$ nm)	2.20	*Angew. Chem. Int. Ed.*, 2014, **53**, 5107–5111
Au_{vertex}–Cu_2O HNCs	25 v/v% methanol	300 W Xe lamp ($\lambda > 400$ nm)	28.87	*J. Am. Chem. Soc.*, 2016, **138**, 15766–15773
Hot dog-Au NR@Cu_2O@TiO_2	0.01 M NaOH + 0.0125 M glucose	300 W Xe lamp	105.1	*Nano Energy*, 2017, **33**, 469–475
Au_{vertex}–Cu_2O–$Ag_{5.9}$ HNCs	25 v/v% methanol	300 W Xe lamp ($\lambda > 400$ nm)	122.93	**This work**